Kinematic and intrinsic dipole of cosmic radio background from sky areas observed by SKA and comparison with other dipole estimations

Carlo Burigana & Tiziana Trombetti

INAF-Istituto di Radioastronomia

CMB dipole

COBE

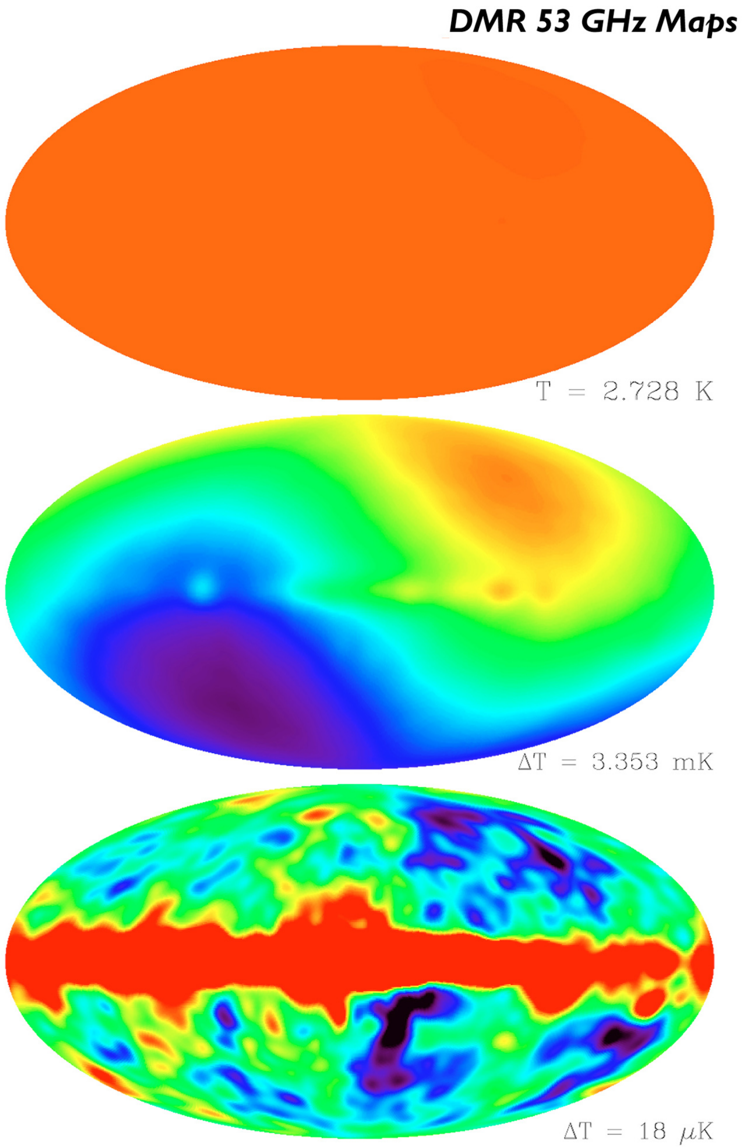

https://lambda.gsfc.nasa.gov/product/cobe/more_images/cobeslide29.jpg

WMAP

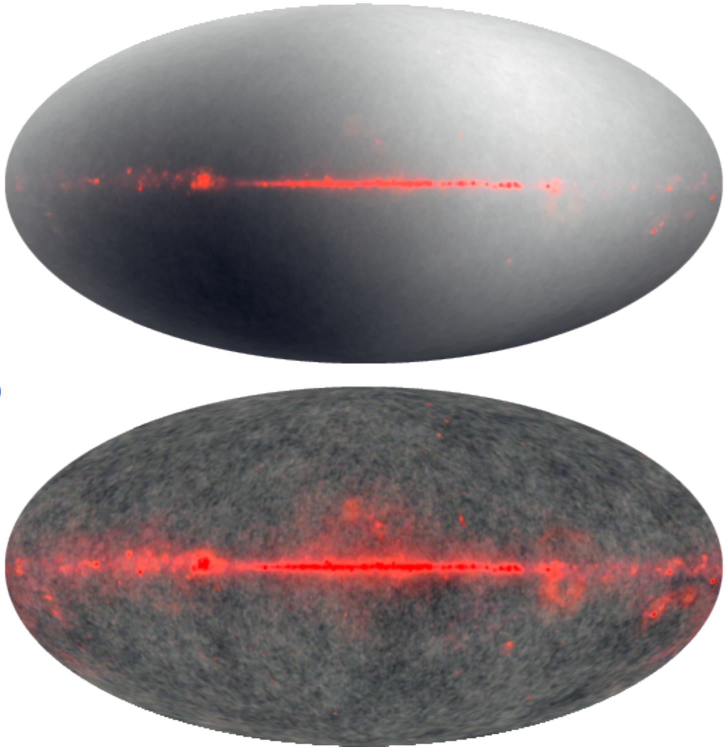

False color images. Q-band red, V-band green, W-band blue. A CMB therm spectrum grey.

Top: 3 color combination image from the Q-, V-, and W-band maps. Dipole and high Galactic latitude anisotropy are seen.

Bottom: similar but without dipole.

https://lambda.gsfc.nasa.gov/product/wmap/pub_papers/firstyear/basic/wmap_cb1_images.html

CMB dipole: *Planck*

Dipole direction in Galactic coordinates

***l*=264.021°, *b*=48.253°   v = (369.82 ± 0.11) km/s**

$\boldsymbol{\beta} = v/c \simeq 1.2336 \times 10^{-3} \simeq A_{dip} / T_0$

velocity of the Solar System barycentre with respect to the CMB

Planck Collaboration 2020, AA 641 A1

First confirmation of v with aberration & modulation (Challinor & van Leeuwen 2002, Sollom 2010) of CMB anisotropies

v= 384 km/s ± 78 km/s (stat.) ± 115 km/s (syst.)

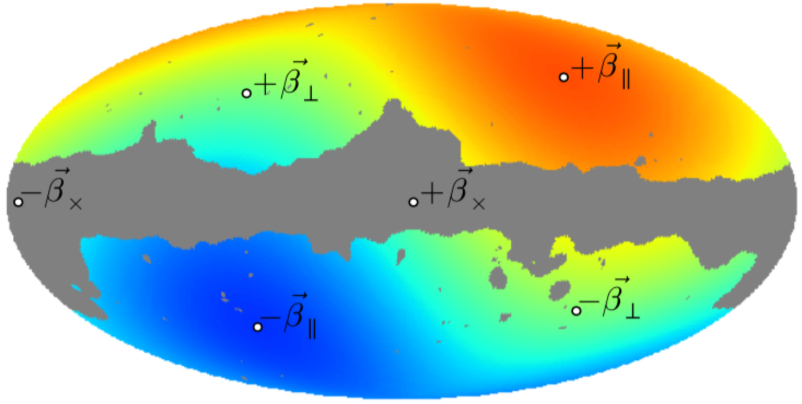

Fig. 2. Specific choice for the decomposition of the dipole vector $\boldsymbol{\beta}$ in Galactic coordinates. The CMB dipole direction $(l, b) = (263^\circ.99, 48^\circ.26)$ is given as $\boldsymbol{\beta}_\parallel$, while two directions orthogonal to it (and each other) are denoted as $\boldsymbol{\beta}_\perp$ and $\boldsymbol{\beta}_\times$. The vector $\boldsymbol{\beta}_\times$ lies within the Galactic plane.

Planck Coll. 2014, A&A 571, A27, Planck 2013 results. XXVII. Doppler boosting of the CMB:

Eppur si muove

- ❑ **We observe the CMB dipole, and we now firmly known from *Planck* that a significant part of it is kinetic**

But … is it almost fully kinetic or there is also a non negligible intrinsic dipole?

For many standard models the anisotropy power of intrinsic dipole and quadrupole is expected to be similar … but ...

- ✓ **CMB space missions observed a relatively low quadrupole (and also other types of low multipole anomalies)**
- ✓ **But, in principle, anisotropy power of intrinsic dipole may be larger**

CMB vs matter dipole

Many galaxy surveys indicates that:
matter dipole ≠ CMB dipole
See e.g. N.J. Secrest + 2022, ApJL 937, L31
A Challenge to the Standard Cosmological Model

In this meeting, see also talks by D. Schwarz, S. von Hausegger, G.F. Lewis

NRAO VLA Sky Survey (NVSS; Condon et al. 1998)

Wide-field Infrared Survey Explorer (WISE; Wright et al. 2010)

- ✓ The large dipoles seen in radio galaxies & quasars independently reject, at 2.6σ & 4.4σ, the null hypothesis that the dipoles arise from Doppler boosting and relativistic aberration with velocity 370 km/s in the CMB dipole direction
- ✓ Dipole amplitudes are about 3 and 2 times larger than the respective kinematic expectations and point 45° and 26° from CMB dipole $(l=264.021^{\circ}, b=48.253^{\circ})_{CMB}$
- ✓ The joint significance of this rejection of the cosmological principle is 5.1σ
- ✓ These anomalously large dipoles are statistically consistent with a single, shared dipole of distant galaxies and quasars, with amplitude $\mathcal{D}=(1.40\pm0.13)\times10^{-2}$ in the direction (l, b)=(233°±6°, 34°±5°)
- ✓ No evidence for a frequency dependence of the amplitude
- ✓ Agreement between radio galaxy & quasar dipoles improves by subtracting standard kinematic expectation: $\mathcal{D}=(0.86\pm0.14)\times10^{-2}$; (l, b)=(217°±10°, 20°±7°)
- ✓ Intrinsic overdensity of galaxies and quasars on very large scales, in a direction 48° away from the CMB dipole

Future CMB space missions

Proposals & concepts for CMB spectrum:

Early space missions ideas:
Diffuse Microwave Emission Survey (DIMES), Kogut 1996, 0.5 ≲λ≲15 cm;
FIRAS II, Fixsen and Mather 2002, λ ≲ 1 cm

Sub-orbital experiments: Balloon Interferometer for Spectral Observations of the Universe (BISOU); Cosmic Spectroscopy Mission (COSMO)

Primordial Inflation Explorer (PIXIE), Kogut et al. 2011, proposed to NASA

Polarized Radiation Interferometer for Spectral disTortions and INflation Exploration (PRISTINE), ESA F-mission call, Cosmic Vision 2015–2025

FOSSIL, FTS fOr CMB Spectral diStortIon expLoration, A proposal to the ESA M7 call, Aghanim, N. et al. 2022

White papers:
ESA "Voyage 2050":
J. Chluba et al., 2019, New Horizons in Cosmology with Spectral Distortions of the Cosmic Microwave Background, arXiv:1909.01593
Astro2020 US Decadal Survey: J. Chluba et al., 2019, Spectral Distortions of the CMB as a Probe of Inflation, Recombination, Structure Formation and Particle Physics, arXiv:1903.04218, 2019BAAS...51c.184C

Almost definitive CMB large missions (anisotropy T&P extreme sensitivity and arcmin resolution, spectrum absolute measurements)

Polarized Radiation Imaging and Spectroscopy Mission (PRISM)
André, P., et al. 2014, JCAP 2014, Issue 02, id. 006 – For ESA Call

White paper submitted in answer to the "Voyage 2050" call (long term plan - ESA science programme):
Microwave spectro-polarimetry of matter and radiation across space and time, J. Delabrouille et al. 2021, Experimental Astronomy, 51, 1471 (arXiv:1909.01591)

See http://tiny.cc/ESA-2050 for ESA positive answer

"In the middle" …

Anisotropy T&P with possible extension to spectrum absolute measurements

PICO: Probe of Inflation and Cosmic Origins,
S. Hanany et al., 2019, arXiv:1908.07495, 2019BAAS...51g.194H

Differential

Pioneering proposal …
B-Pol: detecting primordial gravitational waves generated during inflation
De Bernardis, P., Bucher, M.; Burigana, C.; Piccirillo, L. for B-Pol Coll., Experimental Astronomy, 23, p. 5-16
ESA Cosmic Vision 2015-2025 Call

Lite (Light) Satellite for the studies of *B*-mode polarization and Inflation from cosmic background Radiation Detection
LiteBIRD. Approved for launch in 2027
Ishino+ 2016, Proc SPIE, 9904, id 99040X - ISAS, JAXA
~ degree resolution

Almost definitive CMB mission for anisotropy T&P

Cosmic ORigins Explorer,
Delabrouille, J., et al. 2018. Exploring cosmic origins with CORE: Survey requirements and mission design.
JCAP 2018, Issue 04, id. 014
(last version, proposed several times to ESA, with variants)
Set of JCAP papers

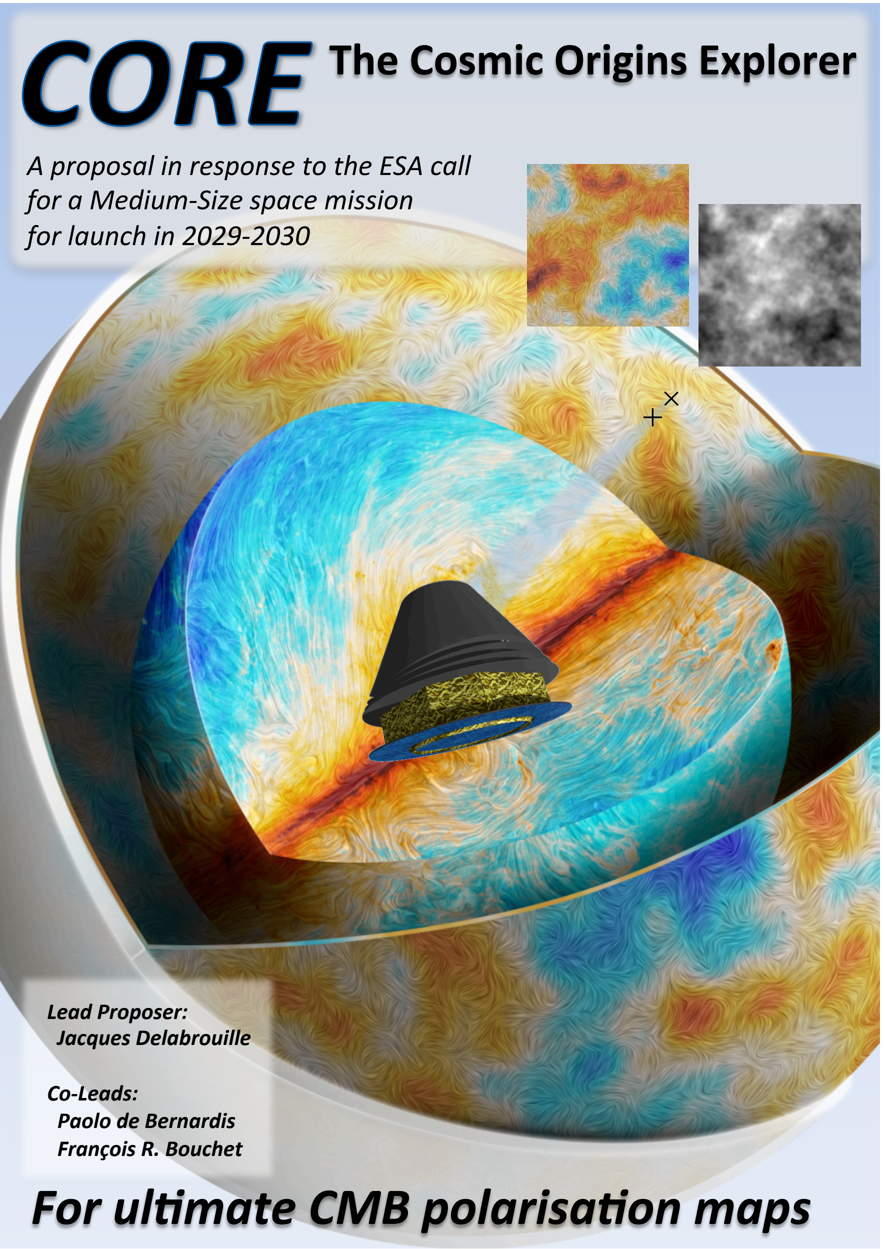

TABLE 1 | Proposed CORE-M5 frequency channels and performance.

Channel [GHz]	Beam [arcmin]	N_{det}	ΔT [μK.arcmin]	ΔP [μK.arcmin]	ΔI [μK_{RJ}.arcmin]	ΔI [kJy sr^{-1}.arcmin]	$\Delta y \times 10^6$ [y_{SZ}.arcmin]
60	17.87	48	7.5	10.6	6.81	0.75	−1.5
70	15.39	48	7.1	10	6.23	0.94	−1.5
80	13.52	48	6.8	9.6	5.76	1.13	−1.5
90	12.08	78	5.1	7.3	4.19	1.04	−1.2
100	10.92	78	5.0	7.1	3.90	1.2	−1.2
115	9.56	76	5.0	7.0	3.58	1.45	−1.3
130	8.51	124	3.9	5.5	2.55	1.32	−1.2
145	7.68	144	3.6	5.1	2.16	1.39	−1.3
160	7.01	144	3.7	5.2	1.98	1.55	−1.6
175	6.45	160	3.6	5.1	1.72	1.62	−2.1
195	5.84	192	3.5	4.9	1.41	1.65	−3.8
220	5.23	192	3.8	5.4	1.24	1.85	...
255	4.57	128	5.6	7.9	1.30	2.59	3.5
295	3.99	128	7.4	10.5	1.12	3.01	2.2
340	3.49	128	11.1	15.7	1.01	3.57	2.0
390	3.06	96	22.0	31.1	1.08	5.05	2.8
450	2.65	96	45.9	64.9	1.04	6.48	4.3
520	2.29	96	116.6	164.8	1.03	8.56	8.3
600	1.98	96	358.3	506.7	1.03	11.4	20.0
Array		2,100	1.2	1.7			0.41

The CORE sensitivity for temperature anisotropy measurements in given terms of equivalent thermodynamic (or CMB) temperature, as in the case of polarization anisotropy measurements, and also in terms of antenna (or RJ) temperature, intensity and SZ effect Comptonization parameter y. The sensitivity is estimated assuming $\Delta\nu/\nu = 30\,\%$ bandwidth, 60 % optical efficiency, total noise of twice the expected photon noise from the sky and the optics of the instrument being at 40 K. The second column gives the FWHM resolution of the beam. This configuration has 2,100 detectors, about 45 % of which are located in CMB channels between 130 and 220 GHz. Those six CMB channels yield an aggregated CMB sensitivity of 2 μK.arcmin (1.7 μK.arcmin for the full array). Reprinted from Burigana et al. (2018) [©SISSA Medialab Srl. Reproduced by permission of IOP Publishing. All rights reserved].

Specifications

CORE like differential CMB mission

Summary of simulations

Predicted improvement

in the recovery of CMB distortion parameters

with respect to FIRAS

for different assumptions on calibration & foreground (relative) residuals at various angular scales

E_{cal} and E_{for} at scale given by N_{side} — **Results derived with approach (c)**

		E_{cal}	E_{for}	CIB amplitude	Bose-Einstein	Comptonization
Ideal case, all sky		–	–	$\simeq 4.4 \times 10^3$	$\simeq 10^3$	$\simeq 6.0 \times 10^2$
$N_{side}=64$	All sky	10^{-4}	10^{-2}	$\simeq 15$	$\simeq 42$	$\simeq 18$
$N_{side}=64$	P76	10^{-4}	10^{-2}	$\simeq 19$	$\simeq 42$	$\simeq 18$
$N_{side}=64$	P76ext	10^{-2}	10^{-2}	$\simeq 17$	~ 4	~ 2
$N_{side}=64$	P76ext	10^{-4}	10^{-2}	$\simeq 22$	$\simeq 47$	$\simeq 21$
$N_{side}=64$	P76ext	10^{-4}	10^{-3}	$\simeq 2.1 \times 10^2$	$\simeq 2.4 \times 10^2$	$\simeq 1.1 \times 10^2$
$N_{side}=64$	P76ext	$10^{-3}_{(\leq 295)}$–$10^{-2}_{(\geq 340)}$	10^{-2}	$\simeq 19$	$\simeq 26$	$\simeq 11$
$N_{side}=64$	P76ext	$10^{-3}_{(\leq 295)}$–$10^{-2}_{(\geq 340)}$	10^{-3}	$\simeq 48$	$\simeq 35$	$\simeq 15$
P76ext, $N_{side} = 128$		$10^{-3}_{(\leq 295)}$–$10^{-2}_{(\geq 340)}$	10^{-2}	$\simeq 38$	$\simeq 51$	$\simeq 23$
P76ext, $N_{side} = 128$		$10^{-3}_{(\leq 295)}$–$10^{-2}_{(\geq 340)}$	10^{-3}	$\simeq 43$	$\simeq 87$	$\simeq 39$
P76ext, $N_{side} = 256$		$10^{-3}_{(\leq 295)}$–$10^{-2}_{(\geq 340)}$	10^{-2}	$\simeq 76$	$\simeq 98$	$\simeq 44$
P76ext, $N_{side} = 256$		$10^{-3}_{(\leq 295)}$–$10^{-2}_{(\geq 340)}$	10^{-3}	$\simeq 85$	$\simeq 1.6 \times 10^2$	$\simeq 73$

3 different approaches

a. Using each of the 19 frequency channels, assuming they are independent (essentially compares the amplitude of dipole of a distorted spectrum with that of the BB, being so sensitive to the overall difference between the two cases)

b. Using the 171 (19 × 18/2) combinations coming from the differences of the maps from pairs of frequency bands (compares the dipole signal at different frequencies for each type of spectrum, being so sensitive to its slope)

c. Combining cases (a) and (b) together

Burigana+ 2018

Several methods to look at intrinsic dipole (i.e. to constrain v)

Typically based on correlations between background anisotropy at different multipoles induced by boosting+aberration

❖ e.g. with CORE (Burigana+ 2018)

✓ Extenting boosting effects to polarization and cross-correlations will enable a more robust determination of purely velocity-driven effects that are not degenerate with the intrinsic CMB dipole: overall S/N ≃ 13

✓ Essentially as an ideal cosmic-variance-limited experiment up to $\ell \simeq 2000$, improving on the Planck detection

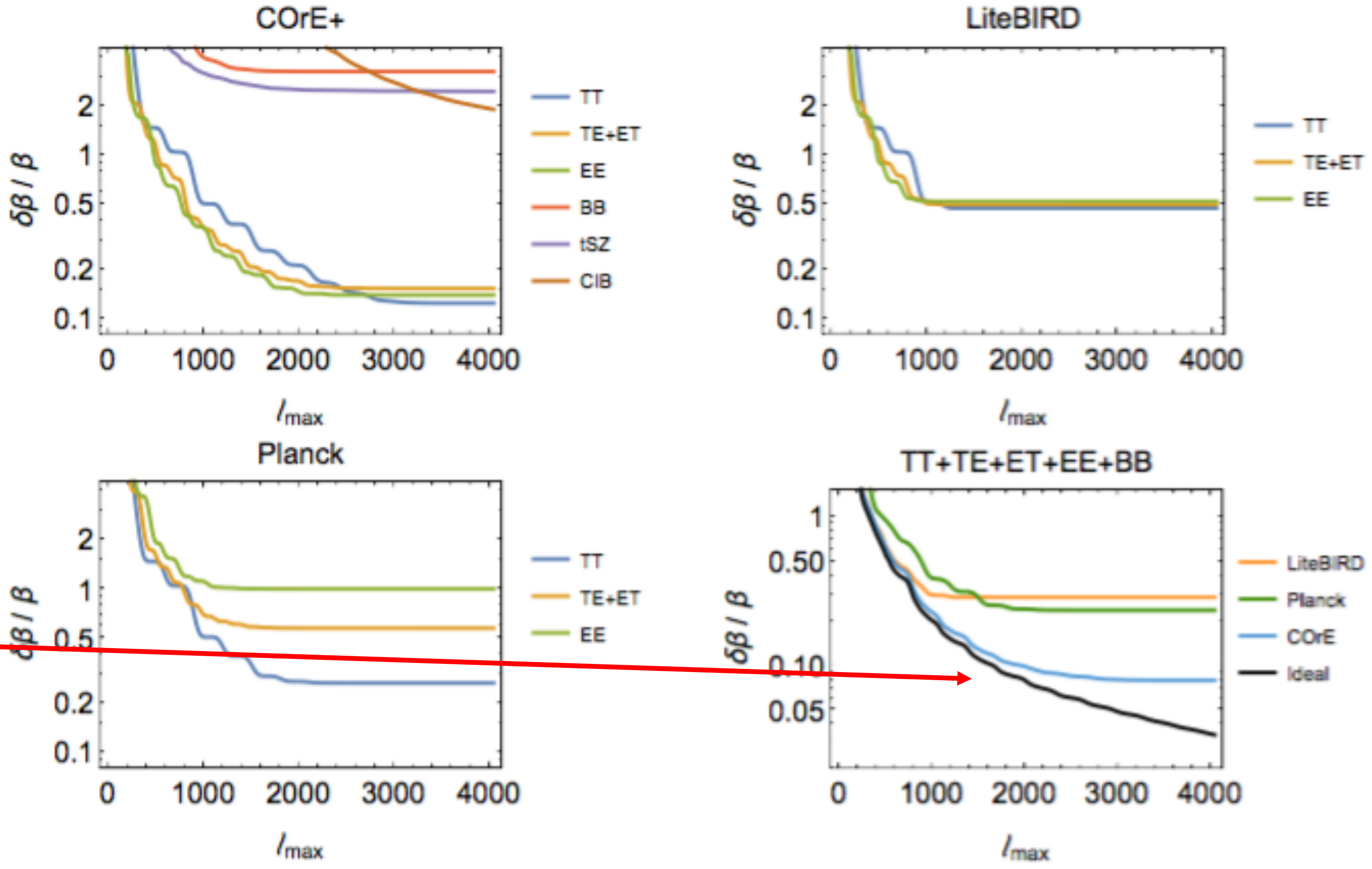

❖ Method based on the exploitation the **leakage of the intrinsic dipole into** the CMB **monopole** and **quadrupole** (Yasini & Pierpaoli 2017)

A proof of concept: CMB distortions & kinetic vs intrinsic dipole

Looking only at the dipole?

If CMB spectrum were a perfect BB, kinetic and intrinsic degenerate

But …
since small spectral distortions are expected to exist?

Assumption:
intrinsic and kinematic dipoles not aligned (opposite possible by chance, but very unlikely)

From Trombetti+ (2021)

z axis // observer velocity

kinetic — intrinsic — Sum over p types of distortions

$$a^{\rm glob}_{1,m}(\nu,\beta) = \Delta a_{1,m}(\nu,\beta) + a^{\rm BB}_{1,m}(\beta) + a_{{\rm BB},1,m} + \sum_{j=0}^{P-1} \tilde{a}_{j,1,m}(\nu),$$

where

$$\tilde{a}_{j,1,m}(\nu) = a_{j,1,m}\left(\frac{\partial T_{\rm th}}{\partial \eta}\frac{\partial \eta}{\partial p_j}\right)_0$$

BB
Superscript: observer motion
Subscript: intrinsic anisotropy

related to the type of distortion
≠ 0 only in the presence of deviations from BB

are 0 for m ≠ 0

(A) If $\tilde{a}_{j,1,m}(\nu) \ll \Delta a_{1,0}(\nu,\beta)$.

In the right system only m=0 shows frequency dependence

If (A) false, they are physically connected & joint analysis of the modes with $m = 0$ and $m \neq 0$, helps, at $m \neq 0$, the discrimination between $\tilde{a}_{j,1,m}(\nu)$ and $a_{{\rm BB},1,m}$.

Observer motion ⟶ modification and transfer of the CB spectrum

$$T_{\rm th}^{\rm BB/dist}(\nu,\hat{n},\boldsymbol{\beta}) = \frac{xT_0}{\ln(1+1/(\eta(\nu,\hat{n},\boldsymbol{\beta}))^{\rm BB/dist})} \quad (1)$$

observed signal map

where $\eta(\nu,\hat{n},\boldsymbol{\beta}) = \eta(\nu')$ with $\nu' = \nu(1-\hat{n}\cdot\boldsymbol{\beta})/(1-\beta^2)^{1/2}$ (2)

Lorentz invariance of photon distribution function $\eta(\nu)$

sky direction unit vector associated to polar coordinates (colatitude) and (longitude)
$\boldsymbol{\beta}$ = v /c

N.B.: monopole background is by definition the isotropic component – no aberration

Compton-Getting effect (Forman, M. A. 1970, Planet. Space Sci., 18, 25)

$$T_{\rm th}^{\rm BB/dist}(\nu,\theta,\phi,\beta) = \sum_{\ell=0}^{\ell_{\rm max}}\sum_{m=-\ell}^{\ell} a_{\ell,m}(\nu,\beta)Y_{\ell,m}(\theta,\phi) \quad (3)$$

$Y_{\ell,m}(\theta,\phi)$ spherical harmonics, related to associated Legendre Polynomial $P_\ell^m(\cos\theta)$

$$Y_{\ell,m}(\theta,\phi) = \tilde{P}_\ell^m(\cos\theta) \qquad \tilde{P}_\ell^m(\cos\theta) = \sqrt{\frac{2\ell+1}{4\pi}\frac{(\ell-m)!}{(\ell+m)!}}P_\ell^m(\cos\theta) \quad (4)$$

renormalized associated Legendre Polynomial **when m=0**

- ✓ We adopt a reference system with the z axis parallel to the observer velocity
- ✓ Adopting a reference system with the z axis parallel (or antiparallel) to the observer velocity, we are interested only in the non-vanishing coefficients with $m = 0$
- ✓ The publicly available tools (e.g. HEALPix, Górski et al. 2005) allow us to efficiently compute the $a_{\ell,m}$ coefficients passing from a reference system to another
- ✓ See Goldstein, J. D. 1984, J. Geophys. Res., 89, 4413 for transformations of spherical harmonics coefficients under rotation

Azimuthal symmetry simplification

Solution in terms of derivatives

T. Trombetti+ 2024

Let us assume that $T_{th}^{BB/dist}(w)$ with $w = \cos\theta$ can be expanded in Taylor's series around $w = \cos(\pi/2)=0$

i.e. the direction perpendicular to observer motion;

$T^{(0)}_{th}$, T'_{th}, …, $T^{(6)}_{th}$ derivatives with respect to w evaluated at $w = 0$

$$a_{0,0} = \sqrt{4\pi}\left[T^{(0)}_{th} + \frac{1}{6}T''_{th} + \frac{1}{120}T^{(4)}_{th} + \frac{1}{5040}T^{(6)}_{th}\right]$$

monopole: observed ≠ intrinsic

$$a_{1,0} = \sqrt{\frac{4\pi}{3}}\left[T'_{th} + \frac{1}{10}T'''_{th} + \frac{1}{280}T^{(5)}_{th}\right],$$

$$a_{2,0} = \frac{1}{3}\sqrt{\frac{4\pi}{5}}\left[T''_{th} + \frac{1}{14}T^{(4)}_{th} + \frac{1}{504}T^{(6)}_{th}\right],$$

$$a_{3,0} = \frac{1}{15}\sqrt{\frac{4\pi}{7}}\left[T'''_{th} + \frac{1}{18}T^{(5)}_{th}\right],$$

$$a_{4,0} = \frac{1}{105}\sqrt{\frac{4\pi}{9}}\left[T^{(4)}_{th} + \frac{1}{22}T^{(6)}_{th}\right],$$

$$a_{5,0} = \frac{1}{945}\sqrt{\frac{4\pi}{11}}\,T^{(5)}_{th},$$

$$a_{6,0} = \frac{1}{10395}\sqrt{\frac{4\pi}{13}}\,T^{(6)}_{th},$$

Separation: odd / even ℓ & derivatives

≈ Danese & De Zotti 1981 but there using θ=0 and $\theta=\pi/2$

$$D_\ell = (2\ell - 1)D_{\ell-1}, \text{ with } D_0 = 1$$

denominator in front of square root

Signal given with respect to ν

Link between derivatives respect to w with derivatives with respect to ν

$$\nu' = \nu(1 - \beta w)/(1 - \beta^2)^{1/2}$$

$$\frac{dT_{th}}{dw} = \frac{dT_{th}}{d\nu'}\frac{d\nu'}{dw} = \frac{dT_{th}}{d\nu'}\frac{-\beta\nu}{(1-\beta^2)^{1/2}}$$

$-\beta\nu/(1-\beta^2)^{1/2}$ does not contain w,

$$\frac{dT^n_{th}}{dw^n} = \frac{dT^n_{th}}{d\nu'^n}\left[\frac{-\beta\nu}{(1-\beta^2)^{1/2}}\right]^n$$

Approximate scaling as β^n

Changing β

For a speed $\beta_a \neq \beta$ (ex. $\beta_a > \beta$), defining $f_a = \beta_a/\beta$ (ex. $f_a > 1$), the ratio between the derivatives computed for these two speeds is:

$$\frac{T^{(n)}_{th}\big|_{\beta}}{T^{(n)}_{th}\big|_{\beta_a}} = f_a^{-n}\left(\frac{1-\beta_a^2}{1-\beta^2}\right)^{n/2} R_n$$

$$R_n = \left(\frac{dT^n_{th}}{d\nu'^n}\bigg|_{\nu'_{\beta,\perp}}\right)\left(\frac{dT^n_{th}}{d\nu'^n}\bigg|_{\nu'_{\beta_a,\perp}}\right)^{-1} \simeq 1$$

Cosmic Background Spectrum

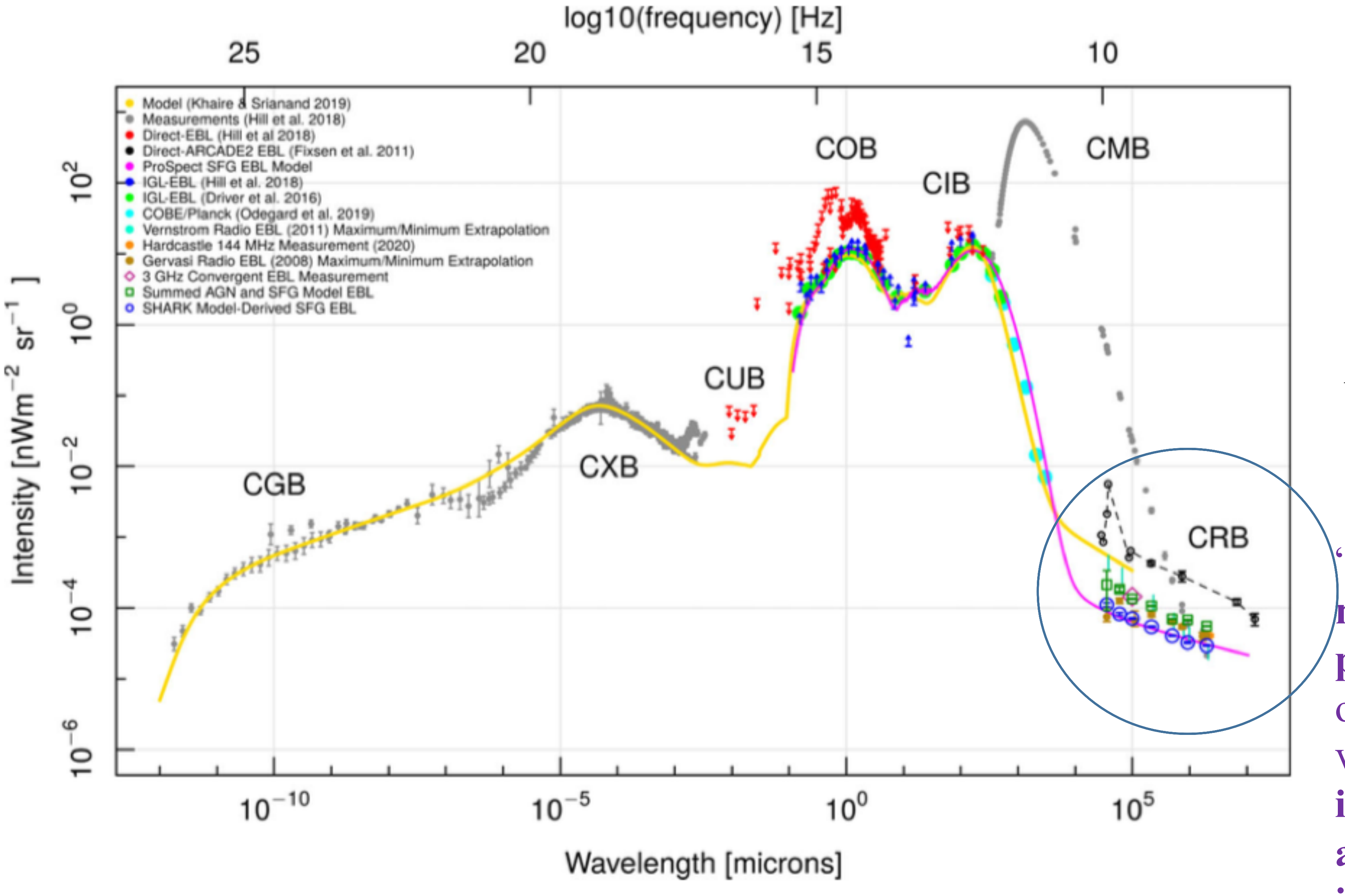

Figure 7. The complete EBL over the entire measured EM range, including our discrete radio source count measurements along with those from the literature (as indicated in the legend). Also shown is the CMB contribution which dominates at most radio wavelengths and the constraints on the total non-CMB radio EBL from ARCADE2 (black dotted line and open circles). Our model-derived (extrapolated) data points in the radio region are shown as green squares (AGN and SFG) and blue circles (SFG). The solid purple line is the best fitting (dotted) SFG only prediction from Fig. 6.

Tompkins, S. A., et al. 2023, MNRAS, 521, 332

The cosmic radio background from 150 MHz to 8.4 GHz and its division into AGN and star-forming galaxy flux

"We can **rule out a significant missing discrete source radio population** and suggest that the cause of the high ARCADE-2 radio-EBL values may need to be sought **either in the foreground subtraction or as a yet unknown diffuse component in the radio sky**."

Specifications of SKA, precursors, pathfinders, and others

(according to SKA-TEL-SKO-DD-0000002 Rev: 03, SKA1 System Baseline Design V2, P. E. Dewdney et al. 2016)

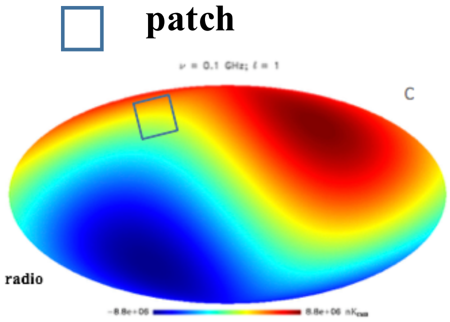

		eMERLIN	JVLA	GBT	GMRT	Parkes MB	LOFAR	FAST
A_{eff}/T_{sys}	m^2/K	60	265	276	250	100	61	1250
FoV	deg^2	0.25	0.25	0.015	0.13	0.65	14	0.0017
Receptor Size	m	25	25	101	45	64	39	300
Fiducial frequency	GHz	1.4	1.4	1.4	1.4	1.4	0.12	1.4
Survey Speed FoM	$deg^2\ m^4\ K^{-2}$	9.00×10^2	1.76×10^4	1.14×10^3	8.13×10^3	6.50×10^3	5.21×10^4	2.66×10^3
Resolution	arcsec	10-150 x 10^{-3}	1.4 - 44	420	2	660	5	88
Baseline or Size	km	217	1 - 35	0.1	27	0.064	100	0.5
Frequency Range	GHz	1.3-1.8, 4-8, 22-24	1 - 50	0.2 - 50+	0.15, 0.23, 0.33, 0.61, 1.4	0.44 to 24	0.03 – 0.22	0.1 – 3
Bandwidth	MHz	400	1000	400	450	400	4	800
Cont. Sensitivity	$\mu Jy\text{-}hr^{-1/2}$	27.11	3.88	5.89	6.13	16.26	266.61	0.92
Sensitivity, 100 kHz	$\mu Jy\text{-}hr^{-1/2}$	1714	388	373	411	1029	1686	82
SEFD	Jy	46.0	10.4	10.0	11.0	27.6	45.2	2.2

		MeerKAT	WSRT	Arecibo	ASKAP	SKA1-low	SKA-mid
A_{eff}/T_{sys}	m^2/K	321	124	1150	65	559	1560
FoV	deg^2	0.86	0.25	0.003	30	20.77	0.49
Receptor Size	m	13.5	25	225	12	35	15
Fiducial frequency	GHz	1.4	1.4	1.4	1.4	0.11	1.67
Survey Speed FoM	$deg^2\ m^4\ K^{-2}$	8.86×10^4	3.84×10^3	3.97×10^3	1.27×10^5	6.49×10^6	1.19×10^6
Resolution	arcsec	11	16	192	7	7	0.25
Baseline or Size	km	4	2.7	225	6	80	150
Frequency Range	GHz	0.7 - 2.5, 0.7 - 10	0.3 – 8.6	0.3 - 10	0.7-1.8	0.050 – 0.350	0.35-14
Bandwidth	MHz	1000	160	1000	300	300	770
Cont. Sensitivity	$\mu Jy\text{-}hr^{-1/2}$	3.20	20.74	0.89	28.89	3.36	0.75
Sensitivity, 100 kHz	$\mu Jy\text{-}hr^{-1/2}$	320	830	89	1582	184	66
SEFD	Jy	8.6	22.3	2.4	42.5	4.9	1.8

Dipole sensitivity on patches

Sensitivity on 2 arcmin pixel,
1 day of integration, 10 or 40 MHz band

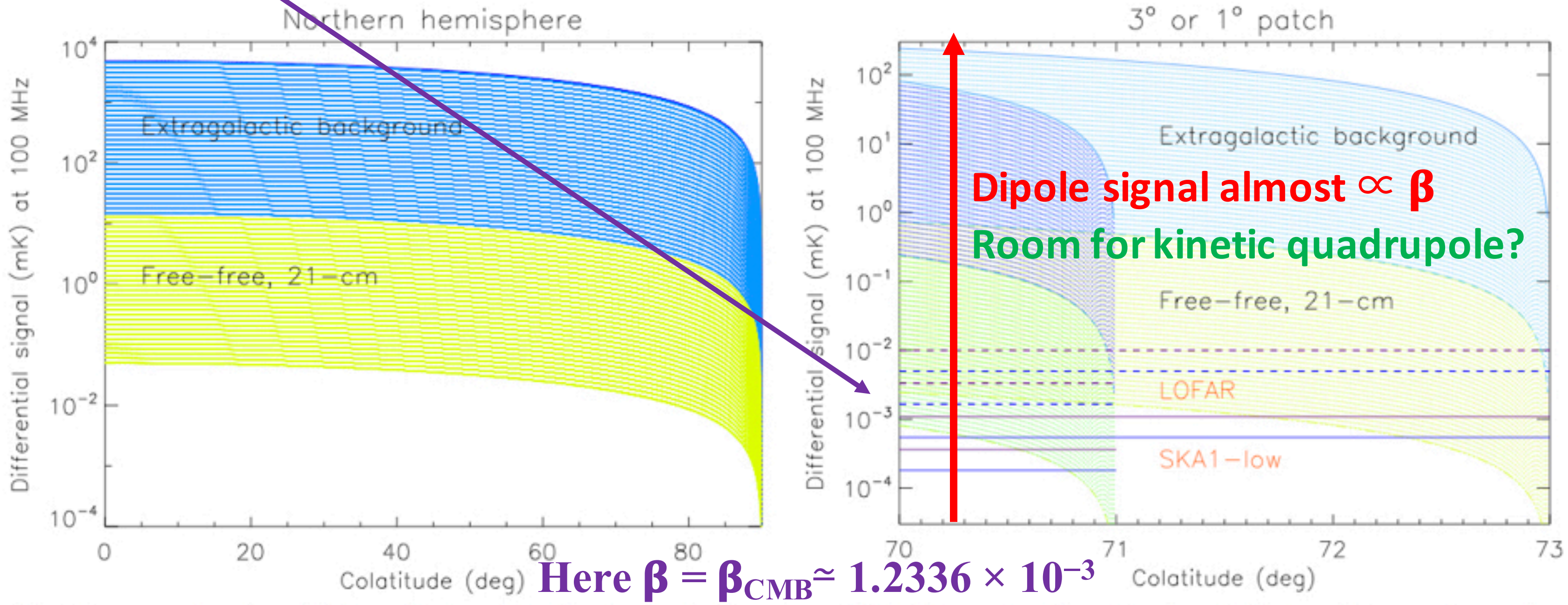

Here $\beta = \beta_{CMB} \simeq 1.2336 \times 10^{-3}$

Fig. 5: Range of predicted differential signal for the dipole, $\Delta T(\theta) = \Delta a_{\ell,0}\,[3/(4\pi)]^{1/2}\cos\theta$, where θ is the colatitude and $\Delta a_{\ell,0}$ refers to the dipole harmonic component ℓ=1, m=0 in a frame with the z-axis parallel to the observer motion, after the subtraction of the standard CMB blackbody, in order to emphasize the interesting signal (here at 100 MHz and in equivalent thermodynamic temperature). The higher part of the blue areas refers to estimates of the signals for the diffuse background from extragalactic radiosources [see e.g. Trombetti+ 2021]; in the lower part it is assumed that sources above certain detection thresholds are subtracted. Yellow areas refer to estimates of the signals for the diffuse free-free distortion, from the minimal prediction accounting for the diffuse IGM contribution to the maximum level corresponding to the integrated contribution from ionized halos, and for various models of the IGM 21-cm redshifted HI line [e.g. Cohen+ 2017]. *Left panel*: the case of an all-sky survey, displayed for simplicity only for a hemisphere. *Right panel*: a zoom of left panel for a patch of 3° (1°); here we display $\Delta T(\theta) - \Delta T(\theta_*)$, with $\theta_* = 73°$ (71°), i.e. the differential signal inside the patch, to be compared with typical sensitivity levels (see also text in Milestones) for LOFAR (dashed lines) and SKA1-low (solid lines) in a nominal pixel of 2 arcmin for one day of integration in the patch. Violet (blue) lines assumes a bandwidth of 10 (40) MHz to appreciate spectral shapes of the 21-cm redshifted HI line (the other types of signal).

Simple estimate: **along a meridian in a reference frame with z-axis parallel to the dipole direction, the signal variation at colatitude θ from a dipole pattern with amplitude ΔT in a limited sky area of linear size Δθ, has an amplitude $|\Delta T_{\Delta\theta}| \simeq \Delta T \cdot (\Delta\theta/90°)\sin\theta$, with $\sin\theta \simeq 1$ at angles large enough from the poles**

- ✓ **Dealing with almost independently observed sky patches (e.g. interferometric techniques)**
- ✓ **In principle, for extreme sensitivities, dipole pattern reconstruction could be carried out not necessarily requiring a coherent sky mapping up to the largest scales [Trombetti & Burigana 2019]**
- ✓ **For example, considering ~50-100 MHz sensitivities to the diffuse signal with forthcoming and future projects**
  - **~ several tens of mK could allow to identify the extragalactic background**
  - **from ~ a few μK to ~ mK it could be possible to study the reionization imprints**

See Trombetti's talk for estimates at @ other SKA frequencies

Sensitivity levels in right panel from Table 1 of Dewdney+ 2016, SKA1 System Baseline Design, SKA Organisation, rescaling the sensitivity in 1 h of integration for a 100 kHz bandwidth

Frequency Range SKA-mid (GHz): 0.35 - 14

Sensitivity @ 100 kHz band
Rescaled to 4 GHz bandwidth @ 10GHz

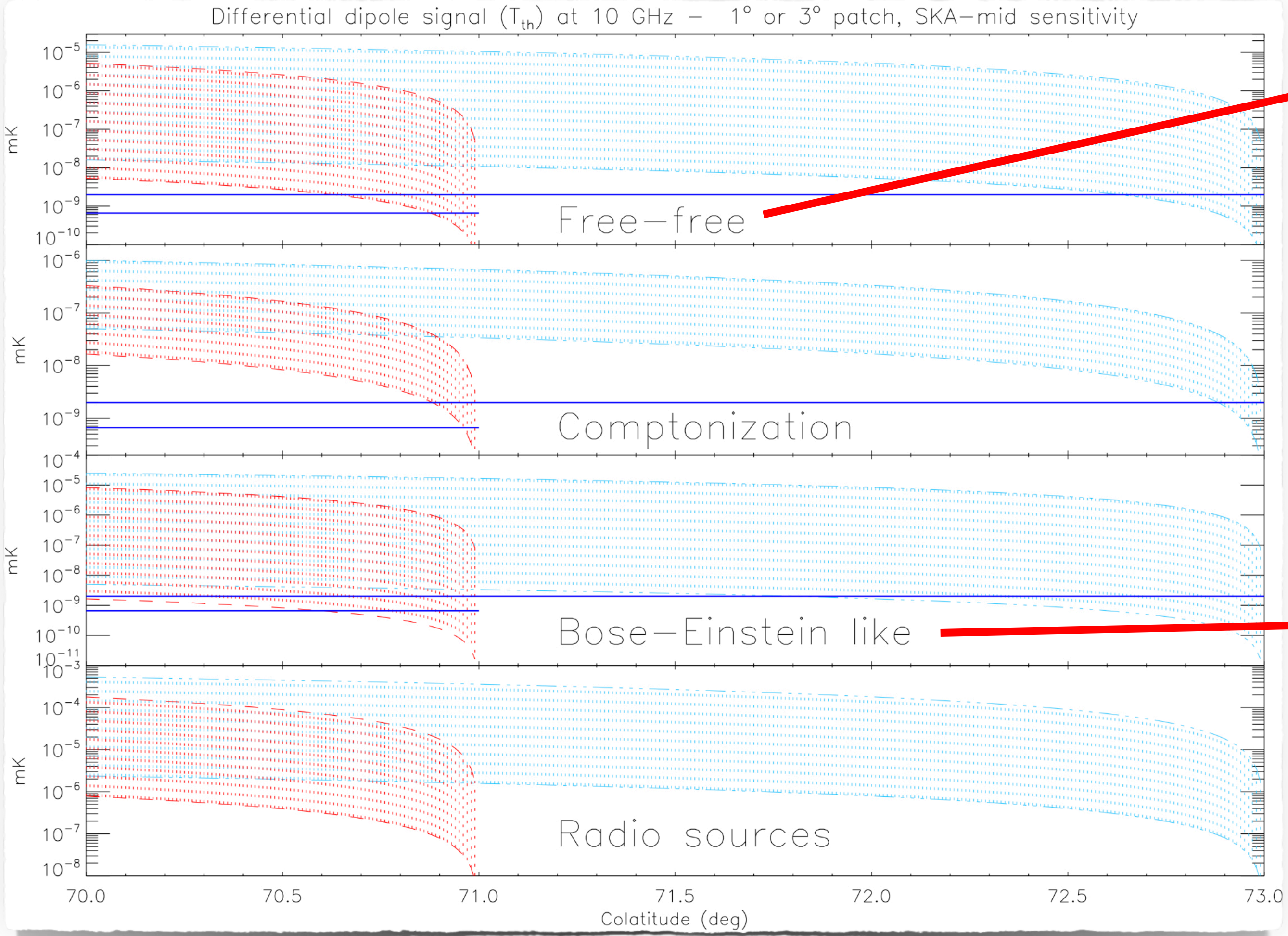

Free-free

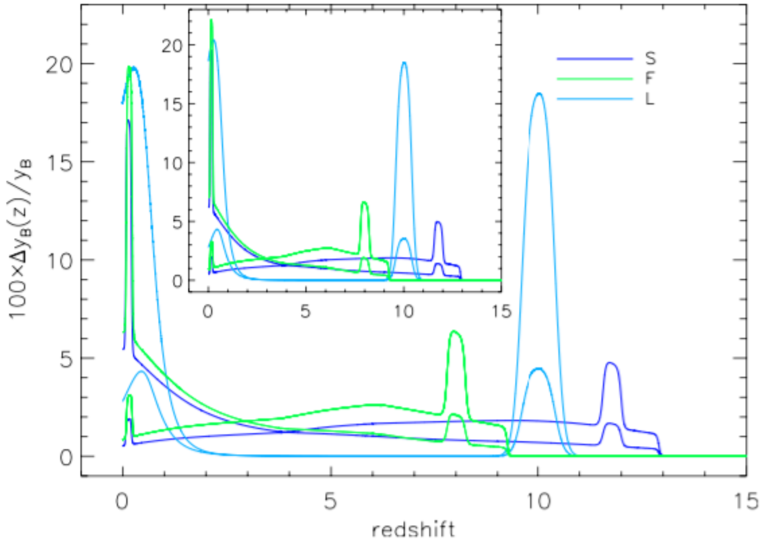

Figure 14. Redshift dependence of the partial contribution to the free–free parameter, evaluated per redshift bin $\Delta z = 0.2$ at each z for $k_{max} = 100$ (and $k_{max} = 500$ in the inset). Being normalized to the global value of y_B at each wavelength, $\Delta y_B(z)/y_B$ turns to be essentially independent of the wavelength, thus we present only the result at 10 cm. The dashed–dotted lines display the results found neglecting the clumping, for the corresponding histories reported in legend.

Trombetti & Burigana 2014

BE: z ~ 10^3 recombination or
z > 10^5 kinetic equilbrium era

Observations & needs

- ✓ ensamble of independent patches, or
- ✓ sky areas from patch assembling with mosaicing techniques to increase differential signal
- ✓ multifrequency (SKA low & mid)

- keeping information on largest scales in the patch or patch assembling (short baselines)

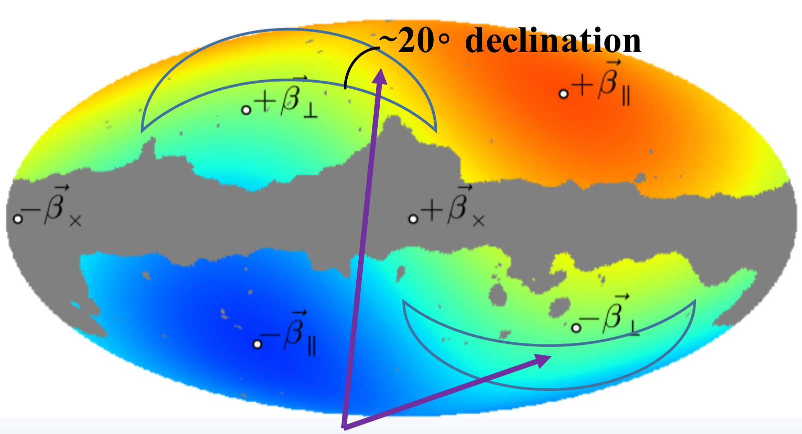

Favourite regions accessible to SKA for patch selection should be far enough from:

- ✓ Galactic plane, to avoid large contamination
- ✓ maximum & minimum of dipole, because $|\Delta T_{\Delta\theta}| \simeq \Delta T \cdot (\Delta\theta/90°)\ \sin\theta$
- ✓ bright sources, to avoid large contamination

- Above sensitivities are based on 1.6 (0.18) min of integration on 2 arcmin pixel of a 1deg (3 deg) side patch

  - ✓ Likely instrument noise dominated
  - ✓ ... but depending on sky area/direction check for source confusion noise

❑ Galactic signal subtraction

- ➢ Galactic modeling
- ➢ Component separation of diffuse signals using multifrequency data (various methods have been elaborated …)
- ➢ Considering more patches to increase statistics and mitigate susceptibility to foreground Galactic modeling (… cosmological signal should come from the same dipole pattern in all patches)

- ➢ Simulations

CMB: nearly all-sky, moderate resolution
SKA: limited sky areas, very high resolution

Conclusions

- **Differential methods relying on precise interfrequency calibration are promising: by using multipole patterns we could significantly improve current limits/measures (without resorting to measurements based on precise absolute calibration or for cross-checking them)**
- **In principle, since CMB spectral distortions exist, intrinsic and kinetic dipoles are not degenerate and precise dipole analyses, looking at the frequency dependence of the m modes, can help to distinguish them**
- **For observations at extreme sensitivity/resolution, the differential method can be extended to sky patches or limited sky areas, as e.g. in the case SKA interferometric observation, for analyses on both background spectra and observer velocity**
- **The CRB is the strongest signal. If extragalactic source number counts will be convergent with SKA at low flux density and it will almost saturate CRB, dipole analyses compared with estimates for various high flux density limits will inform about β**
- **Frequency modulations of CRB dipole spectrum are informative β for other types of signals, tomographic in nature (21cm) or mainly contributed at certain redshifts**